JOURNAL OF Materials CHEMISTRY

Microwave-assisted preparation of uniform pure and dye-loaded $AlPO_4$-5 crystals with different morphologies for use as microlaser systems

Matthias Ganschow,[a] Günter Schulz-Ekloff,[a] Michael Wark,[a] Michael Wendschuh-Josties[b] and Dieter Wöhrle*[c]

[a]*Institut für Angewandte und Physikalische Chemie, Universität Bremen, Leobener Str. NW2, 28359 Bremen, Germany*
[b]*Geowissenschaften-Mineralogie, Universität Bremen, 28359 Bremen, Germany*
[c]*Institut für Organische und Makromolekulare Chemie, Universität Bremen, Leobener Str. NW2, 28359 Bremen, Germany. E-mail: woehrle@chemie.uni-bremen.de*

Received 18th January 2001, Accepted 12th April 2001
First published as an Advance Article on the web 30th May 2001

The study of the influence of the crystal morphology of laser dye-loaded $AlPO_4$-5 molecular sieve on the previously reported laser properties, *i.e.*, laser threshold power density, modes of laser emission and lightfastness, requires synthesis procedures resulting in single crystals of varied length-per-width ratios. The suppression of undesired side-phases ($AlPO_4$-8, VPI-5), as well as the temperature–time field, for the production of pure Rhodamine BE50-loaded crystals with desired uniform morphology by the microwave-heated crystallization method are evaluated and discussed. Uniform plate-like crystals with a thickness of less than 4 μm, for which favorable laser properties can be expected, are obtained only in a small temperature window 150 ± 5 °C with reaction times of about 10 minutes.

Introduction

Molecular sieve materials are characterized by their crystallographically defined framework and their regularly arranged pores. Therefore they are interesting host materials for novel composites based on chromophores in molecular sieves. Dye-containing $AlPO_4$-5 crystals with defined morphologies exhibit various optical properties for prospective applications in microphotonics, like frequency-doubling,[1] laser activity[2,3] or photochromism.[4] The microwave-assisted crystallization of the molecular sieve $AlPO_4$-5 results in the formation of hexagonal barrel-like crystals with a length in the *c* direction of 12 μm and a diameter of the hexagon of 8 μm (8×12 μm),[5] which because of the incorporation of laser dyes into these crystals creates a new class of microlasers.[3] The hexagonal prism of the crystals is perfectly suited to form an optical ring resonator, in which the light circulates by total internal reflection (whispering gallery mode), providing the feedback for the laser action. The laser properties of such composites depend on the size (micrometer range) and shape (hexagonal morphologies) of the crystals in agreement with theoretical predictions, *i.e.*, (i) the number of lines for the laser emission and (ii) the laser threshold power density decrease, if the dimensions of the microcrystals are reduced.[3] Therefore our aim is to get smaller crystals with a desired uniform morphology.

The control of the $AlPO_4$-5 crystallization by the conventional heating method (CV) has been studied repeatedly from the points of view of crystal growth and morphology.[6–8] The $AlPO_4$-5 single crystals, obtained by CV, often exhibit a wide size distribution, different kinds of crystal aggregation and by-products. During the faster microwave-heated (MW) crystallization method very small crystals can be formed since a much higher number of crystal nuclei is simultaneously generated during the rapid increase of the gel temperature and the growth of these nuclei is much more homogeneous.[9] However, frequently, multiple morphologies are present in the synthesis products.[5]

Furthermore, MW crystallization reduces the time for the crystallisation of $AlPO_4$-5 by two orders of magnitude and, thus, enables the incorporation of labile laser dyes which undergo degradation in the conventionally heated hydrothermal process.[5,10]

In the following the synthesis of the microwaved-assisted growth of pure and Rhodamine BE50-containing $AlPO_4$-5 crystals with defined morphology is evaluated for use as microlasers with desired emission properties, *i.e.*, wavelength, irradiance intensity, lasing threshold and stability towards bleeding. The lasing properties will be reported in a subsequent paper.

Experimental

Gel formation

$AlPO_4$-5 molecular sieve was synthesized using pseudo-boehmite (Plural SB, ~75% Al_2O_3, Condea Chemie), orthophosphoric acid (H_3PO_4, 85 wt.%, p.a., Merck), tripropylamine (Pr_3N, Merck) and deionized water as source materials. The batch composition was: $1Al_2O_3 : 1P_2O_5 : 2Pr_3N : 150H_2O$. 4.12 g Al_2O_3 were added to 6.92 g H_3PO_4 in 20 g H_2O under strong mechanical stirring. After 2 min a further 61 g H_2O were added. After 5 min a uniform gel was formed, and then 8.6 g tripropylamine were slowly added under stirring. The pH value of the obtained gel was ~6.8. The agitated gel was aged for 15 h at room temperature. For the encapsulation of the laser dye Rhodamine BE50,[5] the appropriate amount (0.025 mmol) of the dye powder was mixed with the gel at the end of the aging period.

Microwave-assisted crystallization

25 g of the gel was added to a 100 ml Teflon autoclave, which was sealed and placed in the microwave oven (MLS 1200 Mega, Milestone). The synthesis batch was quickly heated (4.5 °C s^{-1}, 1000 W) to 145–170 °C within 1 min and kept at the required temperature for 5–60 min. Then the autoclave was

quench-cooled with iced water. The crystalline product was washed with water and ethanol and dried overnight at 80 °C. Around 0.6–1.0 g product were obtained.

Characterization

The crystallinity of the samples was monitored by X-ray diffraction (Philips PW-1050 X′Change, Cu-$K_{\alpha 1}$, Bragg–Brentano geometry, secondary monochromator), and its morphology was visualized by scanning electron microscopy (ISI-100B, 15 kV).

UV/Vis spectra were recorded in diffuse reflectance mode (Perkin-Elmer Lambda 9). $AlPO_4$-5 without dye was used as a reference standard and barium sulfate was used for calibration. Fluorescence spectra of the colored $AlPO_4$-5 powders were recorded on a Perkin-Elmer LS50 spectrofluorimeter using constant parameters for the optical beam. The excitation wavelength was 470 nm.

The location of the dye molecules in the dye-loaded aluminophosphate crystallites was determined by using optical microscopy.

Results and discussion

Microwave-assisted formation of aluminophosphate phases

By the microwave-assisted reaction different phases and morphologies of aluminophosphate molecular sieves are formed depending on the synthesis temperature and the reaction time. After microwave heating for 15 min at 145 °C a solid product is isolated, consisting, according to X-ray diffraction, of a mixture of molecular sieve phases as well as a small quantity (about 20 mass%) of non-reacted pseudoboehmite Al_2O_3. The crystalline fraction contains $AlPO_4$-8 (AET)[11] and VPI-5 (UFI)[12] needles and a small amount of the characteristic hexagonal $AlPO_4$-5 crystals (Fig. 1). Prolongation of the reaction time results in an increase of the fraction of $AlPO_4$-5 and $AlPO_4$-8 and a decrease in the proportion of the VPI-5 phase. After 40 min of reaction time VPI-5 is no longer observable. VPI-5, formed within the first 15 min, is energetically unstable due to its 18-ring channels and, thus, recrystallizes into the more stable molecular sieve $AlPO_4$-8 possessing only 14-membered rings.[13] Both VPI-5 and $AlPO_4$-8 belong to the class of $AlPO_4$ hydrates, which possess sixfold coordinated Al atoms and are, thus, less stable than the aluminophosphates with only fourfold coordinated Al, of which $AlPO_4$-5 is a member.[14]

If the MW crystallization is carried out at 150 °C, a solid product can be isolated after a shorter reaction time of about 10 min. In addition to minor amounts of non-reacted pseudoboehmite, VPI-5 crystals with needle-like morphology, as well as $AlPO_4$-5 crystals with hexagonal plate-like morphology, are formed (Fig. 2a). The length of the hexagonal plate-like crystals (*c*-direction, parallel to the channel system) is only about 4 μm and, thus, is only about 50% of the diameter in the *ab*-direction of 8 μm (plane perpendicular to the channels).

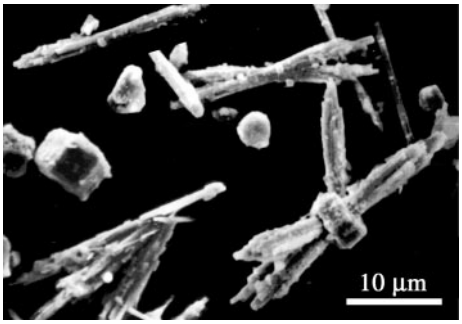

Fig. 1 Scanning electron micrograph of $AlPO_4$-5 and $AlPO_4$-8/VPI-5 crystals (reaction time 15 min, reaction temperature 145 °C).

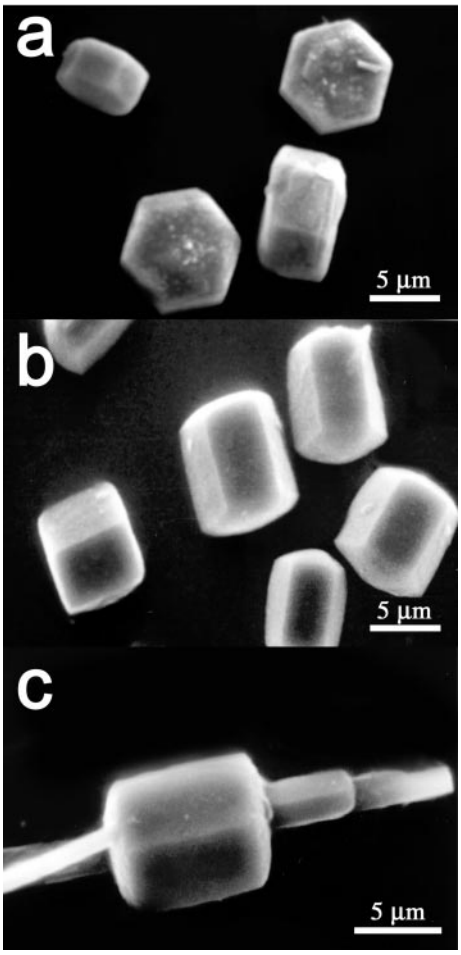

Fig. 2 $AlPO_4$-5 crystals at different reaction times and 150 °C reaction temperature: a) $AlPO_4$-5 crystals 4×9 μm, after 10 min, b) $AlPO_4$-5 crystals 12×9 μm, after 40 min, c) epitaxial growth of $AlPO_4$-5/-8 20×9 μm, after 60 min.

After reaction times longer than about 15 min $AlPO_4$-8, originating from the first precipitated VPI-5, and $AlPO_4$-5 crystals are preferentially formed. Pure $AlPO_4$-5 without any subordinate phases is obtained after 40 min reaction time. Scanning electron micrographs show hexagonal barrel-shaped crystals with a length of about 8 μm in the *c*-direction (Fig. 2b). This means that the plates have changed into hexagonal barrels, where the hexagonal morphology and expansion in the *ab*-plane are retained and only growth in the *c*-direction took place as found by Kodaira *et al.*[9] This kind of behavior has also been reported for several kinds of zeolites using the CV method.[15] A further prolongation of the reaction time to more than 50 min leads to an obviously oriented, probably epitaxial growth of appendages out of the $AlPO_4$-5 bodies in the *c*-direction, *i.e.*, the crystals possess the barrel-like hexagonal body typical of $AlPO_4$-5 with antenna-like appendages attached at its ends in the direction of the *c*-axis (Fig. 2c).

The time-dependent formation and the transient character of the aluminophosphate phases is monitored by scanning electron microscopy (Fig. 2) as well as X-ray diffraction (Fig. 3). At first the formation of different phases at a reaction temperature of 150 °C is discussed. After a reaction time of 10 min the reflections of $AlPO_4$-5 (★) and VPI-5 (+) as well as of pseudoboehmite (#) are detected (Fig. 3). After 5 min, pseudoboehmite is nearly absent, and $AlPO_4$-8 (○) appears instead of VPI-5 (+) due to the VFI→AET phase transition. An additional 15 min later only the pure $AlPO_4$-5 (○) is present, as shown by the X-ray reflections and also the scanning electron micrographs (Fig. 2b). After a total crystallization time of 50 min, reflections of $AlPO_4$-8 (○) reappear (Fig. 3)

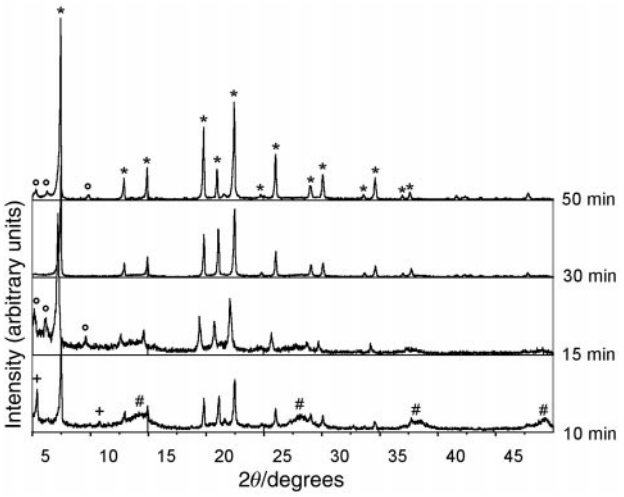

Fig. 3 X-Ray diffractograms of different phases obtained at 150 °C and different reaction times ($AlPO_4$-5 (★), VPI-5 (+), $AlPO_4$-8 (○), pseudoboehmite (#)).

which can be attributed to the grown appendages (Fig. 2c) on the $AlPO_4$-5 barrels, since no other crystals could been observed on the scanning electron micrographs.

At a reaction temperature of 155 °C, transient phases as well as the final formation of the dense phase T-$AlPO_4$, a tridymite analogue of aluminophosphate, are observed.[16] After 5 min reaction time hexagonal disks of $AlPO_4$-5 crystals are detected alongside pseudoboehmite. Subsequently, these disks grow preferentially in the *c*-direction. Only the T-$AlPO_4$ phase appears after a prolonged reaction time (15 min) at 155 °C, and it is the dominant phase after a reaction time of 15 min above 160 °C (Fig. 4). The T-$AlPO_4$ covers previously formed $AlPO_4$-5 crystals (Fig. 5a) or appears exclusively at 170 °C as small spherical crystals with a diameter of 2–5 μm (Fig. 5b). The time-dependent phenomena of transient phase formation are summarized in a temperature–time diagram (Fig. 6).

A tentative interpretation of the initial (Fig. 1) as well as final (Fig. 2c) formation of $AlPO_4$ hydrate phases might be based on plausible considerations (i) of the transient pH values and (ii) of the concentrations of building units in the synthesis mixture. The synthesis starts at a pH value <7,[17,18] *i.e.*, under conditions where the aluminium in the building units[19] prefers an octahedral coordination including water molecules,[20] favoring besides $AlPO_4$-5 the additional formation of VPI-5 and $AlPO_4$-8 (Fig. 1). The synthesis ends with a mixture, which has a low template concentration, so that the pore filling molecule will be water (no incorporation of template in the micropores during crystallization was found for VPI-5[14]), again favoring the

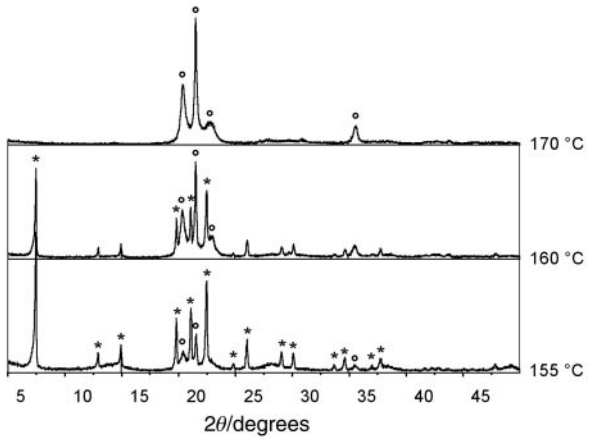

Fig. 4 X-Ray diffractograms, showing the formation of T-$AlPO_4$ (○) and $AlPO_4$-5 (★), after 15 min reaction time at different temperatures.

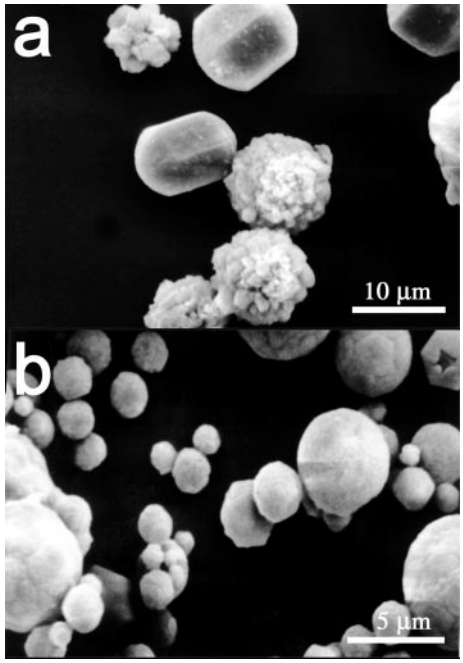

Fig. 5 a) $AlPO_4$-5 crystals covered with T-$AlPO_4$ (8 × 5 μm) after 15 min reaction time at 155 °C reaction temperature and b) T-$AlPO_4$ crystals (2–5 μm) after 15 min reaction time at 170 °C reaction temperature.

formation of $AlPO_4$ hydrate phases, *i.e.*, explaining the preferential appearance of $AlPO_4$-8 (Fig. 2c).

The temporal development of the morphology, *i.e.*, from hexagonal disks (Fig. 2a) to hexagonal prisms (Fig. 2b) occurs as reported previously.[9] The oriented growth of orthorhombic $AlPO_4$-8 on hexagonal $AlPO_4$-5 might be favored by (i) the similar topology of the channels of both structure types and (ii) the nearly identical framework densities.[21]

Rhodamine BE50 incorporation

The laser dye Rhodamine BE50 was incorporated by crystallization inclusion during the MW crystallization. In general, the morphology of $AlPO_4$-5 is only slightly influenced by the dye, depending on the dye size, charge and dipole moment.[5,22] For the employed Rhodamine BE50 concentrations (see Experimental) no influence on the kind of phase and its morphology could be seen. Dye-loaded crystals exhibit exclusively either a plate-like or a barrel-like hexagonal morphology, if formed at the same reaction times and temperatures as described above for the pure $AlPO_4$-5 phase.

Again, at longer reaction times (150 °C, >40 min) crystals

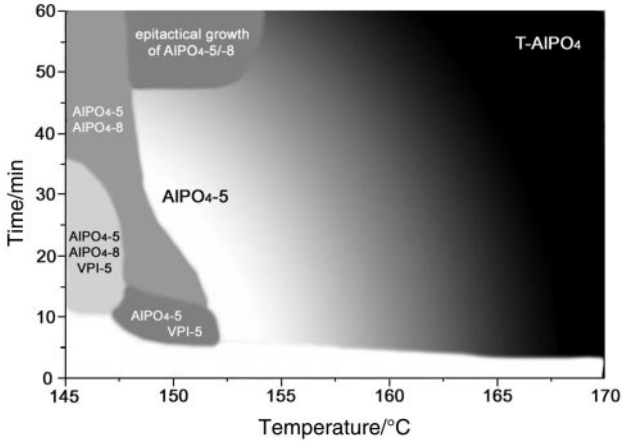

Fig. 6 Reaction temperature- and time-dependent formation of different phases.

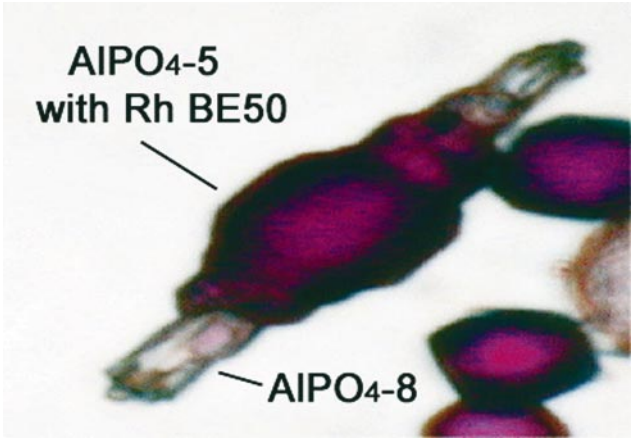

Fig. 7 Optical microscope picture of an epitaxial growth of $AlPO_4$-5/-8 with embedded Rhodamine BE50.

possessing antennae are formed. An analysis of the mixed crystals by optical microscopy shows that only the hexagonal bodies are intensely colored, whereas the antennae are colorless, *i.e.*, the pink Rhodamine BE50 is incorporated only in $AlPO_4$-5 crystals, whereas $AlPO_4$-8 crystals do not host any dye (Fig. 7). The synthesis of $AlPO_4$-5 has no template specificity, since it can be prepared with more than 20 different templates.[6,14] In $AlPO_4$-5 organic templates act as pore fillers and show only weak van der Waals interactions with the framework atoms.[23] In the formation of $AlPO_4$ hydrates, such as VPI-5 and $AlPO_4$-8, water molecules act only as micropore fillers. The introduction of charged molecules, *e.g.* organic templates or dyes, into the micropores is expected to disturb the specific water structures, such as the triple helix structure of water molecules present in the micropores of VPI-5.[24] This explains (i) why no incorporation of organic molecules into the micropores during crystallization was found for VPI-5[14] and (ii) why $AlPO_4$-8 antennae are free of dye molecules.

The optical properties of the laser dye encapsulated in the plate-like morphologies are the same as those observed for Rhodamine BE50 encapsulated in hexagonal barrel-like $AlPO_4$-5 crystals.[5] The strong fluorescence intensities of included Rhodamine BE50 dye prove the encapsulation of monomers, because rhodamine dimers do not fluoresce. A strong host–guest interaction in the dye-loaded $AlPO_4$-5 is obvious from the marked shifts in the absorption and fluorescence spectra (Fig. 8) (absorption/fluorescence maxima of Rhodamine BE50 in aqueous solution are at 557/582 nm; when encapsulated in $AlPO_4$-5 they are at 550/608 nm).[5] In particular, the strong increase of the shoulder at 527 nm of the absorption band for the encapsulated dye in comparison with the dye in aqueous solution is indicative of such an interaction. The strong shoulder at 527 nm in the principal absorption band

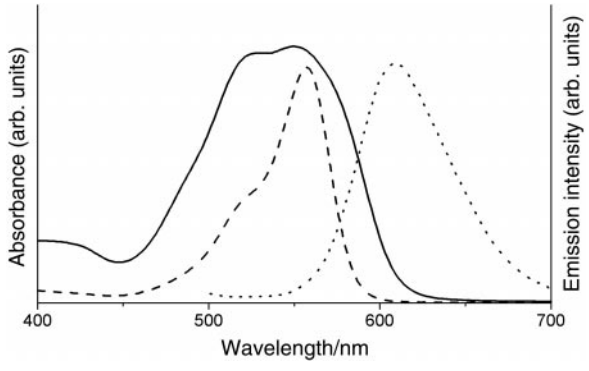

Fig. 8 Diffuse absorption (—) and emission spectra (···) of encapsulated Rhodamine BE50 and absorption of Rhodamine BE50 in aqueous solution (- - -).

for the encapsulated dye originates from the increased probability for transitions from the vibrational ground state of the electronic ground state to an excited vibrational state of the excited electronic state of a monomer, *i.e.*, 0–1 transitions according to the Franck–Condon principle.

Conclusions

The synthesis of thin hexagonal plate-like $AlPO_4$-5 crystals is described for the first time. Under microwave-heated crystallization pure and homogenous plate-like crystals with a thickness of less than 4 μm are only obtained in a small temperature window of 150 ± 5 °C with reaction times of about 10 minutes. Upon longer reaction times the crystals grow preferentially in the *c*-direction resulting in the formation of barrel-like $AlPO_4$-5 crystals. Finally, a long reaction time (>45 min) leads to an obviously oriented, probably epitaxial growth of $AlPO_4$-8 crystals out of the barrel-like hexagonal $AlPO_4$-5 bodies in the *c*-direction.

The laser dye Rhodamine BE50 was incorporated monomerically by crystallization inclusion during the synthesis. No changes of the crystallization parameter in comparison with pure $AlPO_4$-5 are found. The laser dye Rhodamine BE50 is encapsulated in the $AlPO_4$-5 phases only and not in the occasionally appearing $AlPO_4$ hydrates.

Acknowledgements

The project was funded by the Deutsche Forschungsgemeinschaft (Schwerpunkt "Nanoporöse Kristalle"; AZ: SCHU 426/10-3). We gratefully acknowledge the recording of the scanning electron micrographs by Mrs. A. Toltz (Universität Bremen).

References

1 J. Caro, G. Finger, J. Kornatowski, J. Richter-Mendau, L. Werner and B. Zibrowius, *Adv. Mater.*, 1992, **4**, 273.
2 U. Vietze, O. Krauß, F. Laeri, G. Ihlein, F. Schüth, B. Limburg and M. Abraham, *Phys. Rev. Lett.*, 1998, **81**, 4628.
3 I. Braun, G. Ihlein, F. Laeri, J. U. Nöckel, G. Schulz-Ekloff, F. Schüth, U. Vietze, Ö. Weiß and D. Wöhrle, *Appl. Phys. B*, 2000, **70**, 335.
4 K. Hoffmann, F. Marlow and J. Caro, *Adv. Mater.*, 1997, **9**, 567.
5 M. Bockstette, D. Wöhrle, I. Braun and G. Schulz-Ekloff, *Microporous Mesoporous Mater.*, 1998, **23**, 83.
6 S. T. Wilson, in *Introduction to Zeolite Science and Practice*, ed. H. van Bekkum, E. M. Flanigen and J. C. Jansen, Elsevier, Amsterdam, *Stud. Surf. Sci. Catal.*, 1991, vol. 58, p. 137.
7 S. Qin, W. Pang, H. Kessler and J. L. Guth, *Zeolites*, 1989, **9**, 440.
8 H. Kessler, J. Patarin and C. Schott-Darie, in *Advanced Zeolite Science and Applications*, ed. J. C. Jansen, M. Stöcker, H. G. Karge and J. Weitkamp, Elsevier, Amsterdam, *Stud. Surf. Sci. Catal.*, 1994, vol. 85, p. 75.
9 T. Kodaira, K. Miyazawa, T. Ikeda and Y. Kiyozumi, *Microporous Mesoporous Mater.*, 1999, **29**, 329.
10 I. Braun, G. Schulz-Ekloff, M. Bockstette and D. Wöhrle, *Zeolites*, 1997, **19**, 128.
11 J. W. Richardson and E. T. C. Vogt, *Zeolites*, 1992, **12**, 13.
12 M. E. Davis, C. Montes, P. E. Hathaway and J. M. Garces, in *Zeolites: Facts, Figures, Future*, ed. P. A. Jacobs and R. A. van Santen, Elsevier, Amsterdam, *Stud. Surf. Sci. Catal.*, 1989, vol. 49A, p. 199.
13 E. T. C. Vogt and J. W. Richardson, *J. Solid State Chem.*, 1990, **87**, 469.
14 J. A. Martens and P. A. Jacobs, in *Advanced Zeolite Science and Applications*, ed. J. C. Jansen, M. Stöcker, H. G. Karge and J. Weitkamp, Elsevier, Amsterdam, *Stud. Surf. Sci. Catal.*, 1994, vol. 85, p. 653.
15 F. Fajula, in *Guidelines for Mastering the Properties of Molecular Sieves: Relationship between the Physicochemical Properties of Zeolitic Systems and their Low Dimensionality*, ed. D. Barthomeuf, E. G. Derouane and W. Hölderich, Plenum, New York, 1990, p. 53.
16 O. W. Flörke, *Z. Kristallogr.*, 1967, **125**, 134.
17 G. Finger, J. Richter-Mendau, M. Bülow and J. Kornatowski, *Zeolites*, 1991, **11**, 443.

18 X. Ren, S. Komareni and D. M. Roy, *Zeolites*, 1991, **11**, 142.
19 S. Oliver, A. Kuperman and G. A. Ozin, *Angew. Chem.*, 1998, **110**, 49.
20 J. Livage, in *Advanced Zeolite Science and Applications*, ed. J. C. Jansen, M. Stöcker, H. G. Karge and J. Weitkamp, Elsevier, Amsterdam, *Stud. Surf. Sci. Catal.*, 1994, vol. 85, p. 1.
21 W. M. Meier and D. H. Olsen, in *Atlas of Zeolite Structure Types*, Butterworth-Heinemann, London, 1992.
22 M. Ganschow, M. Wark, G. Schulz-Ekloff and D. Wöhrle, in preparation.
23 J. J. Pluth and J. V. Smith, in *Zeolites: Facts, Figures, Future*, ed. P. A. Jacobs and R. A. Santen, Elsevier, Amsterdam, *Stud. Surf. Sci. Catal.*, 1989, vol. 49B, p. 835.
24 L. B. McCusker, Ch. Baerlocher, E. Jahn and M. Bülow, *Zeolites*, 1991, **11**, 308.